WINDII thermosphere temperature perturbation for magnetically active situations

Chantal Lathuillère, Michel Menvielle

WINDII thermosphere temperature perturbation for magnetically active situations

Chantal Lathuillère
Laboratoire de Planétologie de Grenoble, UJF/CNRS, Grenoble, France

Michel Menvielle[1]
Centre d'Études des Environnements Terrestre et Planétaires, IPSL/CNRS, Saint Maur, France

Received 5 April 2004; revised 11 June 2004; accepted 8 July 2004; published 5 November 2004.

[1] Oxygen red line data obtained by the Wind Imaging Interferometer (WINDII) on board the Upper Atmosphere Research Satellite (UARS) between 1992 and 1995 are used to retrieve thermosphere temperature perturbation associated with magnetic activity. Using a statistical approach, we found maximum temperature perturbations of ~300 K at auroral latitudes. We show that the use of longitude sector magnetic indices allows a better characterization of the perturbation than the usual planetary indices. The magnetic activity dependence in the MSIS-90 and DTM94 empirical models is qualitatively in excellent agreement with our results. However, empirical temperature perturbations are underestimated by ~70%. *INDEX TERMS:* 0358 Atmospheric Composition and Structure: Thermosphere—energy deposition; 0350 Atmospheric Composition and Structure: Pressure, density, and temperature; 2427 Ionosphere: Ionosphere/atmosphere interactions (0335); 2431 Ionosphere: Ionosphere/magnetosphere interactions (2736); *KEYWORDS:* thermospheric temperature, magnetic activity, WINDII O(^{1}D) observations, longitudinal sector indices, thermosphere empirical models, thermosphere temperature response to magnetic activity

Citation: Lathuillère, C., and M. Menvielle (2004), WINDII thermosphere temperature perturbation for magnetically active situations, *J. Geophys. Res.*, *109*, A11304, doi:10.1029/2004JA010526.

1. Introduction

[2] Between 1992 and 1997, the WINDII interferometer on board the UARS satellite acquired a large set of thermosphere data from the O(^{1}S) and O(^{1}D) airglow. Doppler temperature profiles from 180 to 260 km altitude were retrieved from the O(^{1}D) data and compared with modeled temperatures [*Lathuillère et al.*, 2002]. Restricting their analysis to 33 quiet magnetic days, the authors have shown that temperatures predicted by the two semiempirical models DTM94 [*Berger et al.*, 1998] and MSIS-90 [*Hedin*, 1991] were in excellent agreement with the observed latitudinal/local time and solar activity variations of the WINDII temperatures. A first analysis of temperature data during a magnetically disturbed day showed that the observed variations were qualitatively well represented in form by the models but with a largely underestimated amplitude. Furthermore, the authors noticed a great variability of the temperatures from one orbit to another that occurred only during magnetically active periods. On the contrary, during geomagnetic quiet days the great reproducibility of the temperature variation along each orbit allowed them to calculate temperature zonal means.

[3] Let us recall here that the transient variations of the observed geomagnetic field are the sum of regular variations, mainly related to the atmospheric dynamo processes, and irregular variations mostly owing to the energy input in the magnetosphere related, for instance, to magnetosphere storms and substorms. It is important to notice that the terms magnetic quiet or disturbed only refer to irregular variations, that is, indicate the absence or presence of irregular variations, also called geomagnetic activity, respectively.

[4] In a very recent paper, *Knipp et al.* [2004] evaluate the relative contributions of solar extreme ultraviolet (EUV) heating, Joule heating, and particle heating to the global budget of the Earth's upper atmosphere between 1975 and 2002. They show that although auroral heating contributes as a mean to ~17% of the total global upper heating and to a third of its variability, it could eventually rise to ~50% of the total power. Contrarily to the solar EUV heating, the upper thermosphere heating sources associated with geomagnetic activity, Joule, and particle heating are extremely variable in the temporal and spatial domains. It is therefore not unexpected that accounting of the geomagnetic activity by means of planetary magnetic indices, as is actually done in the semiempirical atmospheric models, does not result in an accurate description of the upper thermosphere in the presence of magnetic activity. The longitude dependence of the geomagnetic activity can be monitored by means of the 3-hour longitude sector indices proposed by *Menvielle and Paris* [2001], which monitor the magnetic activity at a

[1] Also at Université Paris Sud XI, Orsay, France.

0148-0227/04/2004JA010526

Table 1. Eight Days Corresponding to Magnetic Disturbed Conditions With the Corresponding Solar Activity and Magnetic Activity and the Eight 3-Hour *Kp* Indices

			3-Hour *Kp*							
Day	Daily F10.7	Daily *Ap*	0000–0300	0300–0600	0600–0900	0900–1200	1200–1500	1500–1800	1800–2100	2100–2400
26 Feb 1992	253	65	3+	3+	4–	4–	4	6+	8	7–
5 Aug 1992	131	35	6–	6–	5	4	4+	2+	3	3–
28 Oct 1992	171	19	4+	3	3+	4	2+	3+	3–	3+
7 Dec 1992	120	16	0+	1+	3	2+	4+	1	2+	5
17 Feb 1993	134	36	2	4	4–	5–	7–	6–	2+	1+
18 Mar 1993	124	18	5	4–	4–	3+	3	2–	2	2+
27 Oct 1993	88	38	4	5–	5–	4+	5	5–	5	4+
2 April 1994	82	53	4–	3	3+	5–	5	5+	7	6+

regional scale: the Northern Hemisphere is divided into five sectors of longitude, and the Southern Hemisphere is divided into four.

[5] In this paper we present a statistical analysis of WINDII O(^{1}D) Doppler temperatures measured during 8 magnetic disturbed days, using a binning of the data as a function of the distance of the measurements to the mean auroral oval. The statistical analysis is done as a function of regional and planetary magnetic indices and compared with semiempirical models.

2. Thermosphere Temperature Perturbation in the Presence of Magnetic Activity

[6] The method employed to retrieve the temperature from the WINDII interferometer observations has been extensively discussed by *Lathuillère et al.* [2002] and is just summarized here. Limb observations from the two WINDII fields of view are used in this work in order to extend the latitude coverage of the observations. Apparent temperatures are deduced from the visibility of the interferometer signal and then inverted to obtain temperature altitude profiles. An average over the altitude range 180 to 260 km is then performed. Finally, temperatures are linearly interpolated along each orbit with a 3° latitude sampling.

[7] Only a sample of WINDII observations of the red line has been used to study the temperatures. Among them, 8 days correspond to magnetic disturbed conditions, that is, having a daily planetary *Ap* index larger than 12. These days are listed in Table 1, with the corresponding solar activity, as given by the solar F10.7 cm flux, and magnetic activity, as given by the *Ap* daily index, and the eight 3-hour *Kp* indices.

2.1. Temperature Perturbation

[8] In order to analyze the impact of magnetic activity on the thermosphere temperature, we need to take out temperature variations associated with latitude, local time, season, and solar cycle. To do so, we compute temperature perturbations by subtracting from observed temperatures those corresponding to quiet magnetic activity, hereafter denoted quiet temperatures. However the WINDII O(^{1}D) measurements are much too sparse to achieve a statistical estimation of these quiet temperatures from the observations. We need to have a model of quiet temperatures. *Lathuillère et al.* [2002] have shown that the MSIS-90 and DTM94 models represent very well the observed WINDII quiet temperatures, within a 100 K bias. (Possible explanations for this bias have been extensively discussed, including a contribution of an instrument visibility calibration error which could not be ruled out besides the great precautions taken during preflight calibration to limit such problems.) We therefore use these two models chosen for the following reasons: MSIS-90 is a model widely used in the academic community, while DTM94 is the model used in France for Earth observation satellite orbit predictions.

[9] The quiet temperatures have been calculated for each altitude and time of WINDII observations using the 3-solar rotation average and previous day F10.7 indices to describe the solar activity but using as input a daily $Ap = 4$ value for MSIS-90 model and a $Kp = 0$ value for the DTM94. Then the altitude averaging and the latitudinal interpolation are performed as for the observations. Finally, a value of 100 K is added to the computed quiet temperatures in order to take into account the bias observed between observed and computed quiet temperatures.

[10] Figure 1 shows the resulting thermosphere temperature perturbations during the 8 days corresponding to disturbed magnetic conditions (see Table 1), plotted as a function of latitude. The figures correspond to the use of MSIS-90 (Figure 1a) and DTM94 (Figure 1b) as the quiet time model. Figure 1 clearly shows that observed thermosphere temperature perturbations are maximum at auroral latitudes in both hemispheres and minimum at equatorial and low latitude. Similarly, their dispersion increases with increasing distance to the equator in both hemispheres. Inspection of data from individual orbits (not shown here) shows that this dispersion results from variations in the geomagnetic conditions from one orbit to the other. It is worth noting here that the temperatures denoted with a superimposed circle correspond to the observations made along three orbits during the most active 3-hour intervals of the most active day: 26 February 1992, 1800–2100 UT (see Table 1).

2.2. Thermosphere Heating Associated With Magnetic Activity

[11] The influence of the magnetic activity on the thermosphere temperature can be described in terms of energy deposition in the auroral zone and heat transport from the auroral zone. The predominant term of the auroral energy deposition, the Joule heating [see, e.g., *Knipp et al.*, 2004], can be monitored by the geomagnetic activity because both the Joule energy deposited in the auroral thermosphere and magnetic activity are signatures of the field-aligned/auroral electrojets current system. Simple relations between the

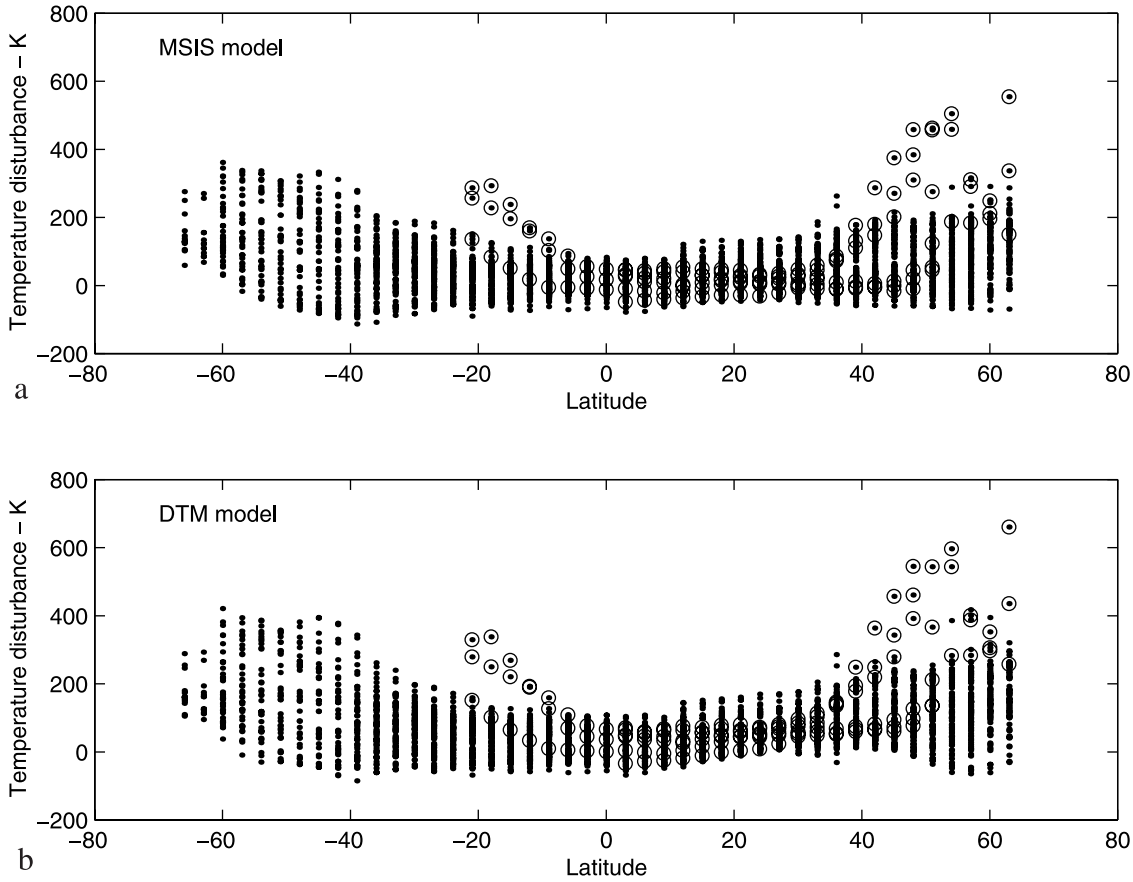

Figure 1. Thermosphere temperature perturbations during the 8 days corresponding to disturbed magnetic conditions. The two figures correspond to quiet temperatures computed using (a) MSIS-90 and (b) DTM-94 models. Circles corresponds to temperature perturbations observed along two orbits during the most active 3-hour interval: 26 February 1992, 1800–2100 UT, *Kp* = 8 (see text for further explanations).

total Joule heating in the Northern Hemisphere and various geomagnetic indices have been proposed [*Knipp et al.*, 2004; *Chun et al.*, 1999; *Ahn et al.*, 1983; *Baumjohann and Kamide*, 1984].

[12] When associated with the development of substorm phenomena, the auroral electrojet variations and associated field-aligned currents are generally maximum in the night sector, and the Joule heating thus depends on local time and accordingly on longitude at a given UT. Joule heating patterns have been modeled as a function of geomagnetic indices [*Foster et al.*, 1983; *Chun et al.*, 2002].

[13] The heat energy transfer through atmospheric convection processes results in a time lag between the energy deposition in the auroral zone and the associated temperature perturbation observed at a point M of latitude θ and longitude λ. The driving parameter of the time lag associated to the heat energy transfer is the distance δ between M and the auroral zone. This time lag is taken into account in the empirical models. DTM94 uses a simple latitude-dependent time delay that ranges from 3 hours at the poles to 6 hours at the equator [*Berger et al.*, 1998]. Such a time lag is also found in Global Circulation Models; for example, during the 2–11 November 1993 magnetic storm, *Emery et al.* [1999] found an 8-hour time lag between the global mean exospheric temperature modeled with the TIEGCM model and the polar cap potential.

2.3. Magnetic Activity Indices

[14] Magnetic indices monitor the irregular variations of the geomagnetic field at the Earth's surface, which are the signature of the currents taking place in the entire magnetosphere as the result of the solar wind-magnetosphere coupling processes. The high degree of complexity of the solar wind-magnetosphere-ionosphere coupling results in a large variety of magnetic signatures, depending upon the state of the magnetosphere, and differing with the geographic and geomagnetic location of the observatory.

[15] Geomagnetic planetary indices *am* and *Kp* aim at monitoring the average magnetic activity intensity at subauroral latitudes (Figure 2). Following *Berthelier* [1993], let us briefly describe the processes of derivation of geomagnetic indices in terms of four components: the measured quantity, the time interval, the network of stations, and the derivation scheme. The reader is referred to *Menvielle and Berthelier* [1991, 1992] and references therein for further details.

[16] 1. The measured quantity is the code *K* derived from the range, measured with respect to the S_R variation of the

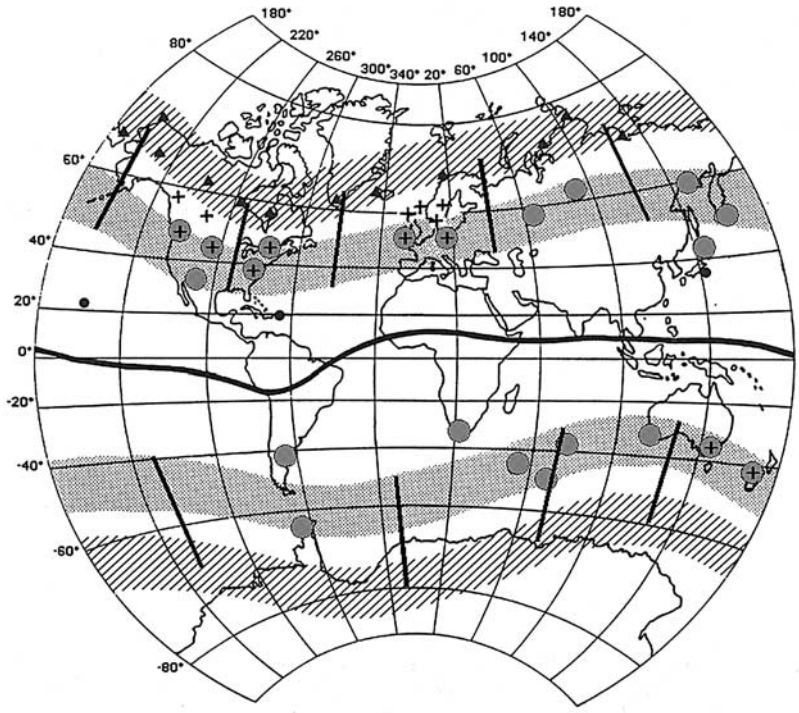

Figure 2. Different networks used in deriving geomagnetic indices: Triangles represent AE, filled circles represent Dst, crosses represent *Kp*, *Ap*, shaded circles for *Am*, *Km*, *a*λ, and circled crosses for stations belonging to both *Kp*, *Ap*, and *Am*, *Km* networks. The average extension of the auroral zone is sketched by the hatched area, that of the subauroral region by the shaded area. Solid lines indicate the position of the dip equator [after *Berthelier*, 1993] and the limits of the longitude sectors.

day under consideration. The S_R can be identified by taking into account the neighboring quiet days and is allowed to have a day-to-day variability. Given the quasi-logarithmic scale used for deriving *K*-indices, the increasing uncertainty in S_R determination with increasing levels of activity does not significantly affect the precision in the *K* determination.

[17] 2. The 3-hour time interval used to derive *K* indices is the best suitable for characterizing geomagnetic activity in subauroral regions (~40 to 55° in magnetic latitude, shaded area on Figure 2). At these latitudes the observed morphology of the irregular variations is actually such that the *K*-equivalent midclass amplitudes are related to the energy density embedded in the irregular geomagnetic variations [*Menvielle*, 1979].

[18] 3. The network of stations is presented in Figure 2. The am network consists of 20 subauroral latitude observatories arranged into groups, each group representing a longitude sector in one of the hemispheres. There are five groups in the Northern Hemisphere and four in the Southern Hemisphere. The *Kp* network consists of 14 observatories: six in Northern America, six in Western Europe, and two in Australia and New Zealand. The resulting obvious limitation in the longitude coverage comes from the distribution of existing observatories that was not truly worldwide at the time of definition of *Kp* [*Bartels*, 1949].

[19] 4. There exist significant differences between the derivation schemes of *Kp* and *am* indices: *am* is obtained from a weighted average of amplitudes corresponding to the midclass range values, with weight evenly distributed according to the longitude of the stations of the present network; it is expressed in nT. On the contrary, *Kp* is the average of standardised codes taken from a quasi-logarithmic scale, with an equal weight given to each station of the initial network. *Kp* is expressed in 3 K units (from 0 to 27); the corresponding amplitude index *Ap*, which can be considered as expressed in 2-nT unit, is deduced from *Kp* by means of conversion tables.

[20] The *K*λ longitude sector indices are computed from the 3-hour range *K* indices scaled at the subauroral observatories of the *am* planetary indice network. In a given longitude sector, the activity is characterized by the average of the *K* measured at the observatories of the sector. The geographical distribution of the am observatories leads to five longitude sector indices for the Northern Hemisphere and four for the Southern Hemisphere (see Figure 2). These indices make it possible to monitor the magnetic activity with regard to both time and longitude [*Menvielle and Paris*, 2001].

3. Results

[21] In this work the observed WINDII thermosphere temperature perturbations at a point *M* of latitude θ and longitude λ are binned with respect to the longitude sector indices (auroral heating at longitude λ characterization) and the distance δ to the auroral zone (heat transport to latitude θ characterization). The longitude sector indices are ranked

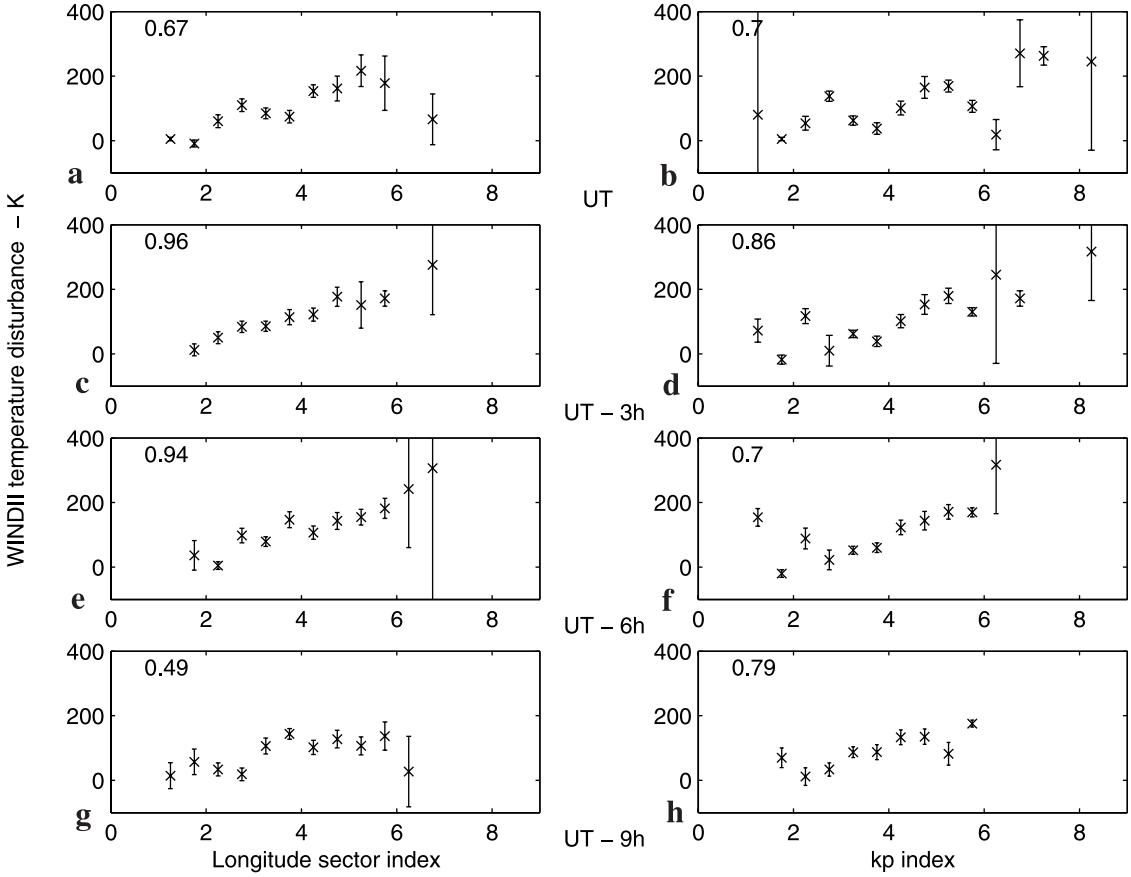

Figure 3. Observed WINDII thermosphere temperature disturbances corresponding to a distance to the auroral oval ranging from 10° to 20°. Values are plotted as a function of geomagnetic activity at a regional scale (as described by the corresponding $K\lambda$ index, left) or a planetary scale (as described by the *Kp* index, right) during four consecutive 3-hour UT intervals: from top to bottom, the ongoing 3-hour UT interval (denoted UT, Figures 3a and 3b), and the three previous ones (denoted UT-3 (Figures 3c and 3d), UT-6 (Figures 3e and 3f), and UT-9 (Figures 3g and 3h)). The numbers in the upper left corners of each figure are the correlation coefficients.

according to the 29 *Kp* classes; the δ values are ranked in six classes, as indicated in the legend of Figure 4. We consider four different time lags (0, 3, 6, and 9 hours) between the energy deposition in the auroral zone and the associated temperature perturbation at latitude θ in the same longitude sector.

[22] Figure 3 presents the observed WINDII thermosphere temperature disturbances, corresponding to the second δ class ($10° < \delta < 20°$) as a function of geomagnetic activity at a regional scale (as described by the corresponding longitude sector index) or at a planetary scale (as described by the *Kp* index) during the ongoing 3-hour interval and the three previous ones. Expected values with 95% confidence intervals are estimated, assuming that the actual data statistical distribution can be considered as a Student one. Large confidence intervals correspond to situations for which we have few temperature perturbation observations.

[23] The eight curves displayed in Figure 3 do not have the same behavior; some of them are not monotonic over the whole range of geomagnetic index values (e.g., the curve corresponding to the planetary activity during the ongoing UT interval, Figure 3a), while some others decreases with increasing geomagnetic activity in the high index value range (e.g., the curve corresponding to the regional activity during the ongoing UT interval, Figure 3b). Regarding the physical processes involved in the heat deposit and transfer in the thermosphere (see section 2), the thermosphere temperature perturbations are expected to regularly increase with increasing geomagnetic activity at a given distance from the auroral zones. We accordingly decided to favor cases corresponding to temperature perturbation smoothly increasing with increasing geomagnetic index values.

[24] According to these simple physics-based a priori criteria, the first conclusion is that a regional monitoring of the geomagnetic activity gives better results than a planetary one. This is clearly illustrated in Figure 3 ($10° < \delta < 20°$) and observed for all the δ ranges we consider. It also appears that the smoother curves correspond to an almost linear temperature perturbation dependence on the index values, when expressed in *K* units. For each δ class we therefore selected the time delay corresponding to the larger correlation coefficient between the temperature perturbation and the geomagnetic index, namely 3 hours for δ smaller than 30° and 6 hours for δ larger than 30°.

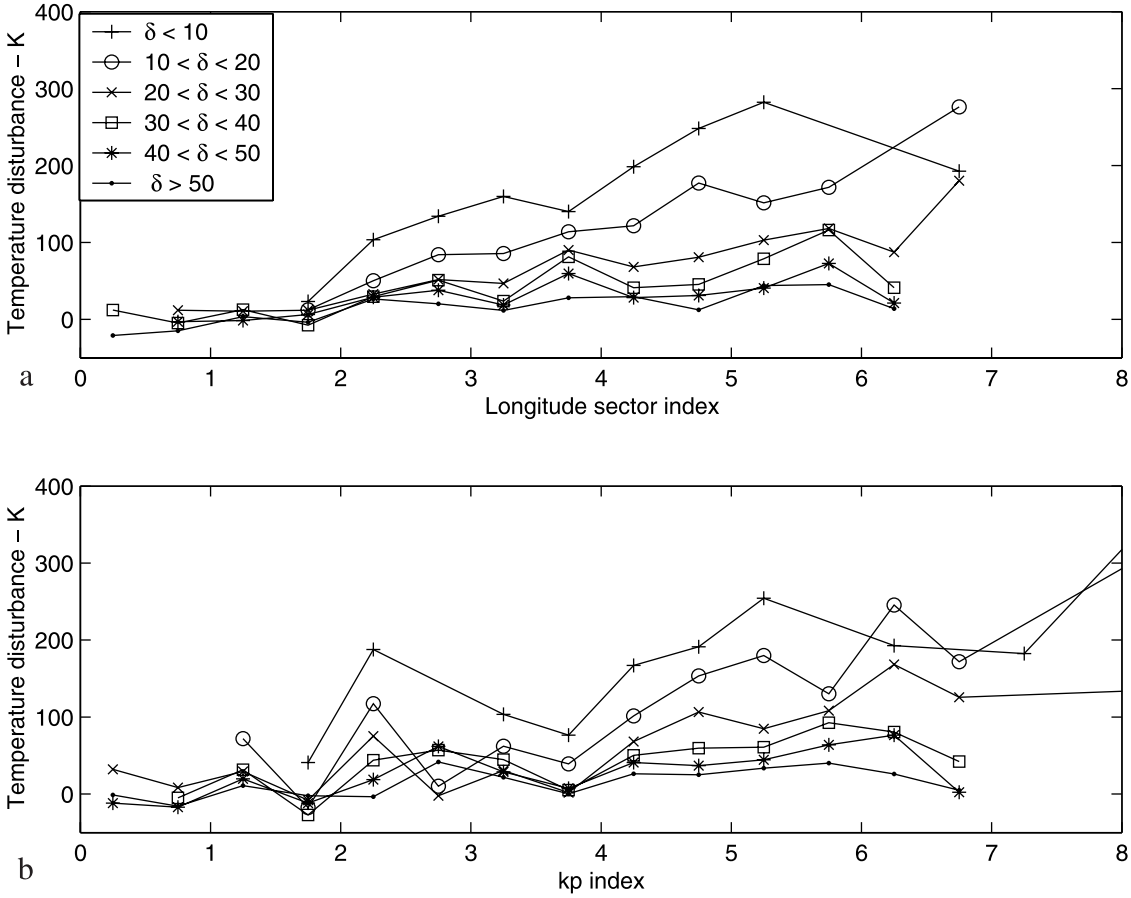

Figure 4. Variations of the thermosphere temperature perturbations as a function of geomagnetic activity. The quiet temperature is computed using the MSIS model (see text for further explanations). The different symbols correspond to the bins of the distance to the auroral oval as indicated in the legend.

Figure 4 summarizes the results we obtain when we use quiet temperatures from MSIS-90 model. In Figure 4a we use a regional monitoring of the geomagnetic activity, while planetary indices are used in Figure 4b. Each curve corresponds to a different bin of distances δ to the auroral oval as indicated in the legend. The increase of temperature with geomagnetic activity ranges from 300 K at auroral latitudes to 10 times less at low latitudes.

[25] Figure 5 presents a comparison between the observed WINDII thermosphere temperature perturbations and the ones we would have obtained from the models. These model temperature perturbations are calculated from the difference between the model temperatures (computed with the relevant magnetic indices) and the quiet temperatures. Figures 5a and 5c correspond to a monitoring of the geomagnetic activity at a regional scale and Figures 5b and 5d correspond to a monitoring at a planetary scale; Figures 5a and 5b correspond to computations made using MSIS-90 model, and Figures 5c and 5d correspond to computations made with the DTM-94 model. In the four cases the graphs show a linear correlation between computed and observed temperature disturbances, which means that the temperature disturbance behavior in the models is in agreement with our observations as already noted by *Lathuillère et al.* [2002] for a selected day. The smaller dispersions and accordingly the larger correlation coefficients are observed for regional monitoring of the geomagnetic activity. It could be therefore interesting to reconstruct the models using the regional indices.

[26] Consider now the two graphs in Figures 5a and 5c. In both cases, the linear correlation between computed and observed temperature is good; it is however slightly better when using MSIS-90 model. The slope of the regression line, given on each graph, is an empirical estimate of the first-order (linear) correction to be made for accounting of the systematic error in the model thermosphere temperature.

4. Conclusion

[27] The results presented in this paper provide a quantitative description of the thermosphere disturbance temperature measured by WINDII during 8 magnetically active days. The magnetic activity is described in terms of K-derived 3-hour indices at the planetary scale and at a regional scale. The data are binned as a function of the distance δ to the auroral oval. Our results show that the more relevant description is obtained when we used regional indices with a time delay of 3-hour interval for δ smaller than 30° and 6 hours for δ larger than 30°. We recall here that our work is based on a very limited set of

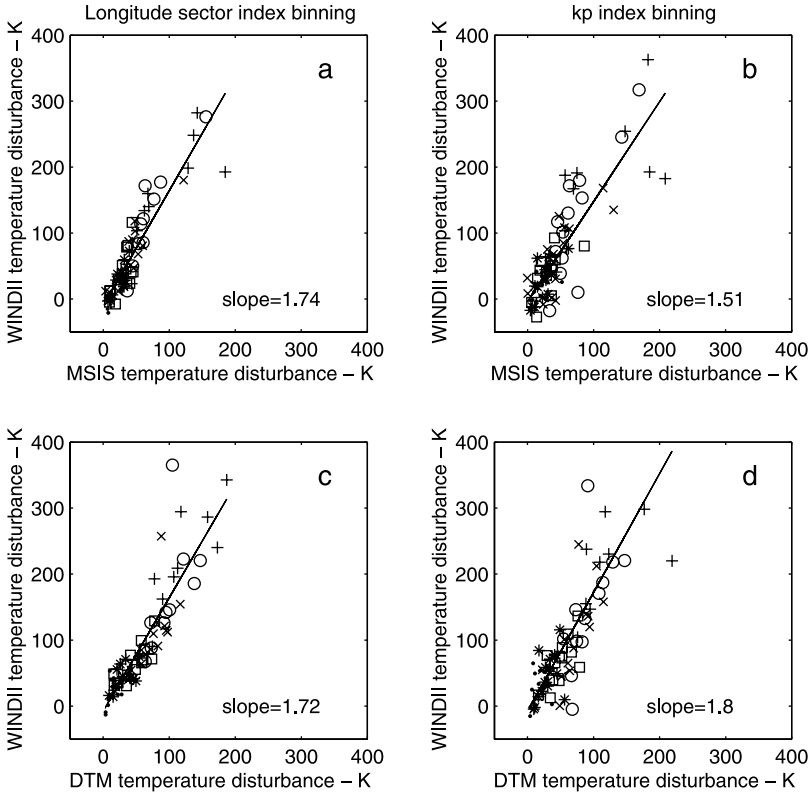

Figure 5. Observed WINDII thermosphere temperature disturbances as a function of computed thermosphere temperature disturbances. The slope of the regression lines are given on each graph. The different symbols correspond to the bins of the distance to the auroral oval as indicated on Figure 4 legend.

observations. Our results have to be confirmed by using other larger data sets enabling one to get better statistics.

[28] Our results also show that thermosphere temperature disturbance estimates provided by the semiempirical models we consider (DTM-94 and MSIS-90) are linearly correlated to our observations but underestimated by ~70%. Lets recall here that both models are mainly based on the same temperature data from OGO-6 and DE-2 satellites. *Berger et al.* [1998] have calculated the variation of the mean ratio between observed and model values as a function of geomagnetic activity. Already in their plot, a trend of higher ratios when magnetic activity increases is clearly seen for the MSIS model. On another hand, they also recall the origins of the limitation of the present thermosphere models; the use of proxy indices to represent energy inputs but also the more basic difficulties of hypotheses never totally satisfied, specifically for magnetically disturbed periods, as the hydrostatic equilibrium and the static diffusive equilibrium. Finally, our results suggest that using a description of the geomagnetic activity at a regional scale, such as that provided by the longitude sector indices, is worth being considered when designing the next generation of semiempirical thermosphere models.

[29] **Acknowledgments.** We would like to acknowledge the members of the WINDII team. The WINDII project was sponsored by the Canadian Space Agency and the Centre National d'Etudes Spatiales (CNES). This research has been supported by the Programme National Soleil-Terre.

[30] Arthur Richmond thanks Douglas Drob and Gordon G. Shepherd for their assistance in evaluating this paper.

References

Ahn, B. H., S. I. Akasofu, and Y. Kamide (1983), The Joule heat production rate and the particle injection rate as a function of the geomagnetic indices *AE* and *AL*, *J. Geophys. Res.*, *88*, 6275–6287.

Bartels, J. (1949), The standardized index, *Ks*, and the planetary index, *Kp*, *IATME Bull. 12b*, IUGG Publ. Off., Paris.

Baumjohann, W., and Y. Kamide (1984), Hemispherical Joule heating and the *AE* indices, *J. Geophys. Res.*, *89*, 383–388.

Berger, C., R. Biancale, M. YII, and F. Barlier (1998), Improvement of the empirical thermospheric model DTM: DTM94—A comparative review of various temporal variations and prospects in space geodesy applications, *J. Geod.*, *72*, 161–178.

Berthelier, A. (1993), The geomagnetic indices: Derivation, meaning and uses in solar terrestrial physics, in *STPW-IV Proceedings*, edited by J. Hruska et al., pp. 3–20, U.S. Govt. Publ. Off., Boulder, Colo.

Chun, F. K., D. J. Knipp, M. G. Mc Harg, G. Lu, B. A. Emery, S. Vennerstrom, and O. A. Trosbichev (1999), Polar cap index as a proxy for hemispheric Joule heating, *Geophys. Res. Lett.*, *26*, 1101–1104.

Chun, F. K., D. J. Knipp, M. G. McHarg, J. R. Lacey, G. Lu, and B. A. Emery (2002), Joule heating pattern as a function of polar cap index, *J. Geophys. Res.*, *107*(A7), 1119, doi:10.1029/2001JA000246.

Emery, B. A., C. Lathuillere, P. G. Richards, R. G. Roble, M. J. Buonsanto, D. J. Knipp, P. Wilkinson, D. P. Sipler, and R. Niciejewski (1999), Time dependent thermospheric neutral response to the 2–11 November 1993 storm period, *J. Atmos. Sol. Terr. Phys.*, *61*, 329–350.

Foster, J. C., J. P. St Maurice, and V. J. Abreu (1983), Joule heating at high latitudes, *J. Geophys. Res.*, *88*, 4885–4896.

Hedin, A. E. (1991), Extension of the MSIS thermosphere model into the middle and lower thermosphere, *J. Geophys. Res.*, *96*, 1159.

Knipp, D. J., T. Welliver, M. G. McHarg, F. K. Chun, W. K. Tobiska, and D. Evans (2004), Climatology of extreme upper atmospheric heating events, *Adv. Space Res.*, in press.

Lathuillère, C., W. Gault, B. Lamballais, Y. J. Rochon, and B. Solheim (2002), Doppler Temperatures from O1D airglow in the daylight thermosphere as observed by the WINDII interferometer on board the UARS satellite, *Ann. Geophys.*, *20*, 203–212.

Menvielle, M. (1979), A possible geophysical meaning of K indices, *Ann. Geophys.*, *35*, 189–196.

Menvielle, M., and A. Berthelier (1991), The K-derived planetary indices: Description and availability, *Rev. Geophys.*, *29*, 415–432.

Menvielle, M., and A. Berthelier (1992), Correction to "The K-derived planetary indices: Description and availability," *Rev. Geophys.*, *30*, 91.

Menvielle, M., and J. Paris (2001), The aλ longitude sector geomagnetic indices, *Contrib. Geophys. Geod.*, *31*, 315–322.

C. Lathuillère, Laboratoire de Planétologie de Grenoble, Bâtiment D de Physique, BP 53, F-38041 Grenoble Cedex 9, France. (chantal.lathuillere@obs.ujf-grenoble.fr)

M. Menvielle, Centre d'Études des Environnements Terrestre et Planétaires, UMR 8639, 4 Avenue de Neptune, F-94100 Saint Maur, France.